Concomitant downregulation of proliferation/survival pathways dependent on FGF-R3, JAK2 and BCMA in human multiple myeloma cells by multi-kinase targeting

Giuliana Cassinelli, Domenica Ronchetti, Diletta Laccabue, Michela Mattioli, Giuditta Cuccuru, Enrica Favini, Valentina Nicolini, Angela Greco, Antonino Neri, Franco Zunino, et al.

Title: Concomitant downregulation of proliferation/survival pathways dependent on FGF-R3, JAK2 and BCMA in human multiple myeloma cells by multi-kinase targeting

Authors: Giuliana Cassinelli, Domenica Ronchetti, Diletta Laccabue, Michela Mattioli, Giuditta Cuccuru, Enrica Favini, Valentina Nicolini, Angela Greco, Antonino Neri, Franco Zunino, Cinzia Lanzi

PII: S0006-2952(09)00492-4
DOI: doi:10.1016/j.bcp.2009.06.023
Reference: BCP 10232

To appear in: *BCP*

Received date: 25-3-2009
Revised date: 28-5-2009
Accepted date: 16-6-2009

Please cite this article as: Cassinelli G, Ronchetti D, Laccabue D, Mattioli M, Cuccuru G, Favini E, Nicolini V, Greco A, Neri A, Zunino F, Lanzi C, Concomitant downregulation of proliferation/survival pathways dependent on FGF-R3, JAK2 and BCMA in human multiple myeloma cells by multi-kinase targeting, *Biochemical Pharmacology* (2008), doi:10.1016/j.bcp.2009.06.023

Concomitant downregulation of proliferation/survival pathways dependent on FGF-R3, JAK2 and BCMA in human multiple myeloma cells by multi-kinase targeting

Giuliana Cassinelli[1], Domenica Ronchetti[2], Diletta Laccabue[1], Michela Mattioli[2], Giuditta Cuccuru[1], Enrica Favini[1], Valentina Nicolini[1], Angela Greco[1], Antonino Neri[2], Franco Zunino[1] and Cinzia Lanzi[1]

[1]Dipartimento di Oncologia Sperimentale e Medicina Molecolare, Fondazione IRCCS Istituto Nazionale dei Tumori; [2]Dipartimento di Scienze Mediche, Università di Milano, Ematologia 1-CTMO, Fondazione IRCCS Policlinico MaRe; [3]Dipartimento di Scienze Biomediche e Tecnologie, Università di Milano, Milano, Italy.

Category: Antibiotics and Chemotherapeutics

Correspondence: Cinzia Lanzi,
Chemotherapy and Pharmacology Unit
Dipartimento di Oncologia Sperimentale e Laboratori
Fondazione IRCCS Istituto Nazionale dei Tumori, via Venezian 1, 20133 Milan, Italy
Phone: 39-02-23902627;
Fax: 39-02-23902692;
E-mail: cinzia.lanzi@istitutotumori.mi.it

Abbreviations:

aFGF, acidic fibroblast growth factor

BCMA, B-cell maturation antigen

BM, bone marrow

GEP, gene expression profile

HMCL, human multiple myeloma cell lines

MM, multiple myeloma

MSC, mesenchymal stromal cell

Abstract

The identification of proliferation/survival pathways constitutively activated by genetic alterations in multiple myeloma (MM), or sustained by the bone marrow (BM) microenvironment, provides novel opportunities for the development of targeted therapies. The deregulated function of protein tyrosine kinases plays a critical role in driving MM malignant phenotype. We investigated the effects of the multi-target tyrosine kinase inhibitor RPI-1 in a panel of human MM cell lines, including t(4;14) positive cell lines expressing the TK receptor FGF-R3. Cells harboring FGF-R3 activating mutations (KMS11 and OPM2) displayed the highest sensitivity to RPI-1 antiproliferative effect. The stimulating effect of the aFGF ligand was abrogated in cells harboring a non-constitutively active receptor. Drug treatment inhibited activation and expression of the FGF-R3^{Y373C} mutant as well as aFGF-dependent signaling involving AKT and ERKs. Inhibition of JAK2, an additional RPI-1 target, resulted in STAT3 inactivation. Blockade of these proliferation/survival pathways was associated with caspase-dependent apoptosis. Moreover, drug treatment abrogated proliferative and pro-invasive stimuli provided by conditioned medium from mesenchymal stromal cells. Gene expression profile of KMS11 cells showed 22 upregulated and 52 downregulated genes upon RPI-1 treatment, with an early modulation of genes implicated in MM pathobiology such as *SAT-1*, *MYC, MIP-1α/β, FGF-R3,* and the growth factor receptor B-cell maturation antigen (*BCMA).* Thus, concomitant blockade of FGF-R3 and JAK2 results in inhibition of several MM-promoting pathways, including BCMA-regulated signaling, and downregulation of disease-associated proteins. These data may have therapeutic implications in the design of treatment strategies resulting in the concomitant inhibition of FGF-R3 and JAK2 signaling pathways in t(4;14) MM.

Key words: BCMA; FGFR3; JAK2; Multiple Myeloma; RPI-1

1. Introduction

Multiple myeloma (MM), which is regarded as an incurable neoplasia, is characterized by clonal expansion of a monotypic plasma cell population in the bone marrow (BM) and induction of osteolytic bone lesions [1]. MM plasma cells harbor chromosome abnormalities most frequently represented by chromosomal translocations involving the IgH locus at chromosome 14 (14q32), which result in the dysregulation of a variety of oncogenes and are significantly associated with shorter survival [2]. The t(4;14) translocation described in 20% of MM patients results in ectopic expression of the fibroblast growth factor receptor 3 (*FGF-R3*) and enhanced expression of *MMSET*, a gene involved in transcription regulation [3-5]. *FGF-R3*, a member of the FGF receptor tyrosine kinase family, has also been found mutated in about 6% of tumors with t(4;14) [1,6]. Although the pathogenic role of *FGF-R3* overexpression in MM has not been clearly defined, the acquisition of kinase-activating mutations appears to confirm its role in the multistage disease process [5,7].

In addition to the tumor genetic background, the BM microenvironment is well recognized as a crucial determinant of the biological and clinical behavior of MM [8]. Extracellular matrix components, stromal cells and secreted growth factors support the malignant growth of MM cells in the BM milieu. The best characterized myeloma growth factor is the cytokine interleukin-6 (IL-6) [9]. However, an increasing number of cytokines, chemokines and cell-to-cell contacts provided by the BM has been found to activate a pleiotropic cascade of proliferative/antiapoptotic signaling pathways including JAK/STAT, PI3K/AKT, RAS/ERK and their downstream components [10]. A better understanding of the profile of signaling pathways involved in the pathophysiology of the disease now provides a framework for the identification of novel targets [1,11]. Accordingly, novel agents recently approved in clinical protocols for MM,

such as bortezomib, thalidomide and analogs, share the ability of targeting tumor-microenvironment interactions as an essential part of their mechanism of action [8,12].

The complex signaling network activated by oncogenic mutations and by the BM microenvironment sustains growth, survival and migration of MM cells contributing to tumor progression as well as to resistance to conventional chemotherapy [1,8]. Since failure to undergo apoptosis has been suggested to play a main role in MM cell accumulation within the BM as well as in drug resistance [9], blocking both intrinsic and BM microenvironment-driven signaling could be required to induce tumor cell death. Multi-targeting approaches represent thereby an attractive therapeutic strategy for MM.

Simultaneous inhibition by small molecule inhibitors of protein tyrosine kinases oncogenically activated in MM cells, and/or regulated by the BM microenvironment, is an attractive therapeutic approach. The 2-indolinone compound RPI-1 was previously described as a multi-target tyrosine kinase inhibitor showing antitumor and antimetastatic/antiangiogenic activity against human tumor models harboring oncogenic RET or overexpressing c-MET [13-18]. In the present study, the effects of the drug were investigated in a panel of human MM cell lines (HMCLs). FGF-R3 and JAK2 were identified as RPI-1 targets mediating antimyeloma activity in vitro. Moreover, expression analysis of drug-treated cells showed the modulation of several key disease-associated genes and proteins including the growth factor receptor B-cell-maturation antigen (BCMA).

2. Materials and Methods

2.1. Cell lines and culture conditions

HMCLs (see Table 1) were obtained from DMSZ-German collection of Microorganisms and Cell Culture, Germany (OPM2, JJN3), or kindly provided by Dr. T. Otsuki (Kawasaki Medical

School, Okayama, Japan) (KMS-28, KMS-18, KMS-11, and KMS-20). They were maintained routinely in Iscove's Modified Dulbecco's Medium supplemented with 10% fetal bovine serum. Multipotent human mesenchymal stromal cells (MSCs) from normal BM adherent cells were kindly provided by Dr. M. Introna (Ospedali Riuniti, Bergamo, Italy) and cultured in Dulbecco's modified Eagle medium, low glucose, with 10% fetal bovine serum. Conditioned medium from MSCs was harvested after 48h of culture in complete medium. The murine fibroblast cell lines NIH3T3 and A6-KMS11 (NIH3T3 stably transfected with the FGF-R3 mutant Y373C) (7) were cultivated in Dulbecco's Modified Eagle's medium with 10% or 5% fetal calf serum, respectively. Cells were incubated at 37°C in a 5% or 10% (fibroblasts) CO_2 atmosphere.

2.2. Drug treatment and biological assays

The synthesis and chemical structure of RPI-1 (1,3-dihydro-5,6-dimethoxy-3-[(4-hydrophenyl)methylene]1-H-indol-2-one) were previously reported [13]. Stock solutions were prepared in DMSO and diluted in culture medium for use (final concentration of DMSO 0.25%, even in controls). Cells were treated with the drug the day after splitting.

Cell viability was assessed by the Trypan blue dye exclusion assay or, alternatively, by the MTT (3-[4,5-dimethylthiazol-2-yl]-2,5-diphenyltetrazolium bromide) assay, measuring dye absorbance at 550 nm. IC_{50} values (drug concentrations producing 50% inhibition) were calculated from dose-response curves. Where indicated, aFGF (50 ng/ml, Sigma Chemical Company, St. Louis, MO) and heparin (100 µg/ml, Serva, Heidelberg, Germany) were added to the cell culture, 24 h after splitting.

Apoptosis was detected by the terminal deoxynucleotidyltransferase-mediated deoxyuridine triphosphate nick-end labeling (TUNEL) assay using the In Situ Cell Detection Kit Fluorescein (Roche, Manheim, Germany) according to the manufacturer's instructions. Samples

were analyzed by flow cytometry using the Cell Quest software (Becton Dickinson, Mountain View, CA).

Invasion assay was performed as previously described [17]. Briefly, cells exposed to vehicle or RPI-1 for 24h, were transferred on a Matrigel-coated (BD Biosciences, San Jose CA) upper chamber of a Transwell system (Costar, Corning Inch., Corning, NY) in serum-free medium. Complete MM medium or conditioned MSCs medium was placed in the lower chamber. The drug was added in both upper and lower chambers at the same concentration used for cell pretreatment. Cells that invaded Matrigel were counted after 24 h of incubation at 37°C. Statistical analyses were performed using Student's 2-tailed t test. P value < 0.05 was considered statistically significant.

2.3. Immunoprecipitation and Western blot analysis

Cells were processed for immunoprecipitation (FGFR3) or total protein extraction followed by Western blotting as previously described [15]. For immunoprecipitation of FGFR3, cell lysates were incubated with pre-swelled protein A-agarose resin (Sigma Chemical Company) and anti-FGFR3 antibody (6 µg for each milligram protein of cell extract), for 2 h at 4ºC. Immunoprecipitates were then washed and eluted as described [15]. For biochemical analysis of FGF-induced effects, cells were previously serum starved for 24 h, treated with RPI-1 for the indicated times, and then stimulated with recombinant human aFGF (50 ng/ml) and heparin (10 µg/ml), in the last 5 min.

The polyclonal antibodies used were: FGFR3 (C-15), STAT3 (K-15), JAK2 (M-126), caspase-9 (H-83) and Mcl-1 (S-19) from Santa Cruz Biotechnology (Santa Cruz, CA); p44/42 ERKs, phospho-JAK2 (Y1007, Y1008) and PARP from Upstate Biotechnology (Lake Placid, NY); phospho-FGF-R (Y653/Y654), phospho-p44/42 ERKs (T202, Y204), phospho-AKT

(S473), phospho-STAT3 (Y705) and cleaved caspase-3 from Cell Signaling Technology (Beverly, MA); caspase-8 and Bcl-X from BD Pharmingen (Franklin Lakes, NJ); AKT from BD Transduction Laboratories (Lexington, KY); survivin and BCMA from Abcam (Cambridge, United Kingdom); actin from Sigma. Monoclonal antibodies were: c-Myc (9E10) from Santa Cruz, Kip1/p27 from BD Transduction Laboratories; phosphotyrosine (pY, clone 4G10) from Upstate, and β-tubulin from Sigma.

2.4. Microarray data analysis

Total RNA extraction and purification, biotin-labeled cRNA synthesis, fragmentation and hybridization on HG-U133A Probe Arrays and arrays scanning were performed as previously described [19,20]. Samples from 3 independent replicas for each time point were profiled. The probe level data were converted to expression values using the MAS 5.0 algorithm, and the normalization was performed using the 'global scaling' procedure, which normalizes the signals of different experiments to the same target intensity. Supervised gene expression analyses were performed using the Gene@Work software platform, which is a gene expression analysis tool based on the pattern discovery algorithm Structural Pattern Localization Analysis by Sequential Histograms (SPLASH). Genes@Work discovered global gene expression 'signatures' that were common to an entire set of at least *n* experiments (the support set), where *n* was a user-selectable parameter called the minimum support [20,21]. Full support and the value of $\delta = 0.02$ were chosen for the analysis. For each gene, the statistical significance of the differential expression across the phenotype and control sets (gene z-score, zg) was computed as previously described [20]. The selected probe list was visualized by means of DNAChip Analyzer (dChip) software [22]. The functional analysis on the selected lists was performed using the Database for

Annotation, Visualization and Integrated Discovery (DAVID) Tool 2008 (U.S. National Institutes of Health)[1] and NetAffx (Affymetrix)[2].

3. Results

3.1. Effects of RPI-1 on HMCLs viability

We investigated the effects of the tyrosine kinase inhibitor RPI-1 on a panel of HMCLs, four of which characterized by aberrant expression of FGF-R3 as a consequence of the t(4;14) translocation (Table 1). Among the t(4;14) positive cell lines, OPM2 and KMS11 harbor FGF-R3 activating mutations, KMS18 has a non-transforming mutation, whereas KMS28 expresses a wild type FGF-R3 [7,23]. Representative dose-response and time-course inhibition curves obtained in cell viability assays are reported in Figures 1A and 1B. OPM2 and KMS11 cells were the most sensitive to the inhibitory effect of RPI-1. The two t(4;14) negative cell lines, KMS20 and JJN3, as well as KMS18 and KMS28 which harbor an FGF-R3 functionally silent in cell culture in basal conditions [7], showed lesser sensitivity (Table 1). However, cell growth enhancement of KMS18 induced by the specific FGF-R3 ligand, aFGF, was abrogated by RPI-1 treatment (Fig. 1C). The additional t(14;16) chromosome translocation present in KMS11 cells [23] did not appear to influence sensitivity to RPI-1, since the same genetic lesion is present in the less sensitive JJN3 cell line.

3.2. Inhibition of FGF-R3^{Y373C} in NIH3T3 transfectants

To determine whether the high sensitivity of KMS11 and OPM2 cells was related to RPI-1 ability to interfere with FGF-R3 oncogenic activation, we first examined the effects of the drug on

NIH3T3 fibroblasts stably transfected with the FGF-R3^{Y373C} mutant present in the KMS11 cell line (A6-KMS11 cells) [7]. Upon treatment with RPI-1, FGF-R3 tyrosine phosphorylation was abolished and its expression was reduced in a dose-dependent manner (Fig. 2A). The drug effect on the receptor levels was confirmed by direct immunoblot detection in whole-cell lysates. Consistent with the abrogation of the receptor oncogenic function, RPI-1 induced a reversion of the transformed morphology of A6-KMS11 cells (not shown).

3.3. Inhibition of FGF-R3- and JAK2-dependent signaling in HMCLs

The effect of RPI-1 was then examined in KMS11 cells expressing endogenous FGF-R3^{Y373C}. As observed in A6-KMS11 fibroblasts, drug treatment resulted in a marked dose-dependent inhibition of the receptor tyrosine phosphorylation and expression (Fig. 2B) which was achieved in the range of antiproliferative drug concentrations (3-30 μM corresponding to IC_{20}-IC_{80}, Fig. 1). Since FGF-R3^{Y373C} maintains biochemical responsiveness to the ligand [7], we examined the effects of RPI-1 on the receptor signaling activation in aFGF-stimulated cells. Tyrosine phosphorylation of FGF-R3^{Y373C} under serum starvation confirmed its constitutive activation (Fig. 2C). Stimulation with aFGF enhanced the receptor signaling as indicated by the increased phosphorylation of the receptor and of the downstream transducers ERKs and AKT. Pretreatment with RPI-1 abolished aFGF-induced activation of FGF-R3^{Y373C}, weakly reduced the receptor expression and inhibited the ligand-induced activation of ERKs and AKT, in a dose-dependent manner (Fig. 2C).

According to previous reports [7,24], the constitutive activation of STAT3 in KMS11 cells was not increased by aFGF stimulation. Nonetheless, STAT3 activation was inhibited by RPI-1 treatment (Fig. 2C) thus suggesting that the drug could affect JAK2, a major receptor-associated tyrosine kinase involved in cytokine intracellular signaling mediated by STAT3 in

myeloma cells including KMS11 [24]. Indeed, drug treatment inhibited JAK2 activation which is constitutive in these cells (Fig. 2D). Both JAK2 and STAT3 were completely dephosphorylated in cells exposed to RPI-1 for 24h, whereas their expression was not affected even with more prolonged treatments (not shown).

3.4. Apoptosis induction

Because activation of signaling pathways dependent on both FGF-R3 and JAK2 is supposed to play a major role in sustaining MM cell survival [9], we examined whether RPI-1 treatment resulted in KMS11 cell death. As determined by TUNEL assay, drug treatment increased the number of apoptotic cells in the KMS11 cell population in a dose-dependent manner (Fig. 3A). Apoptosis was associated with the inhibition of AKT and STAT3 activation and with the downregulation of survivin and the Bcl-2 family member Bcl-X_L (Fig. 3B), known as survival factors in myeloma cells [9,25]. Expression levels of Bcl-2 were not affected by drug treatment (not shown). Likewise, the global expression of Mcl-1, another key regulator of MM survival belonging to the Bcl-2 family [9], was not reduced although an increased detection of two low molecular weight peptides by the anti-Mcl-1 antibody in treated cells (Fig. 3B) suggested the occurrence of truncated pro-apoptotic forms of Mcl-1 [26]. The involvement of both intrinsic and extrinsic apoptotic pathways in cell response to RPI-1 was confirmed by the cleavage of caspases 8, 9, and 3, and of the caspase substrate PARP. These effects were already detectable at 24 h (not shown) and still evident at 72h of cell exposure to the drug (Fig. 3B).

3.5. Gene expression profiling

To gain further insights into the mechanisms of RPI-1 activity in HCMLs, we compared the gene expression profile (GEP) of KMS11 cells prior to and after treatment. The supervised analysis of

GEP data revealed, after 24 h-exposure to RPI-1, a total of 92 probe sets differentially expressed, corresponding to 22 upregulated and 52 downregulated genes (Supplementary Data, Tables 3a and 3b). Functional stratification (Fig. 4) evidenced the downregulation of genes involved in sucrose (*ALDOA*, *SORD*, *ME2*, *GPI*, *PYGB*), fatty acid (*FABP5*, *SCD*, *MECR*), protein (*IARS*), and nucleotide (*PAICS*, *NME1*, and *UCK2*) metabolism, in agreement with a decreased cellular growth. Accordingly, genes devoted to mRNA splicing (*SFRS1-2-3-7*, *SNRPF*), rRNA processing (*RRP9, EXOSC4*), and translation initiation (*EIF1*, *EIF3S8*, *EIF4a1*, *BZW2*) were also significantly downregulated in KMS11-treated cells. In addition, we evidenced the downregulation of genes encoding receptors (*BCMA/TNFRSF17*, *FGFR3*), chaperone proteins (*HSPA8*, *HSP90B1*, *HSPD1*, *HSPE1*), and the transcription factor *MYC*. Conversely, among the overrepresented genes we identified other transcription factors (*JUN*, *JUN-D*, *ATF3* and *KLF4),* and histones. Notably, spermidine/spermine N(1)-acetyltransferase gene (*SAT-1*) and spermidine synthase (*SRM*), two genes involved in the polyamines metabolism, were respectively up- and downregulated.

With the aim of identifying genes and/or pathways early deregulated by RPI-1, we performed the supervised analysis of GEP data from KMS11 samples upon 6 and 15 hours of treatment (Supplementary Data, Tables 1 and 2). Remarkably, analysis at 6h pointed out the downregulation of *MIP-1α* and *MIP-1β* (macrophage inflammatory protein 1-alpha and -beta, chemokine c-c motif ligand 3 and 4) which encode crucial chemokines involved in the development of osteolytic bone lesions as well as in growth, survival and migration in MM [27,28] (Fig. S1 and Table 1b in Supplementary Data). In addition, we found that several histones, splicing factors *(SFRS1-3), SAT1*, *MYC*, and *BCMA,* a B-cell specific TNF receptor family member involved in cell growth and survival regulation of MM [29], were significantly

deregulated starting from 6h of RPI-1 treatment (Fig. 4). *FGF-R3* transcript was significantly downregulated at 15h, although a negative expression trend was already detectable at 6h (Supplementary Data, Fig. S1 and Table 2b). Genes involved in metabolic processes were downregulated starting from 15h, whereas genes encoding heat shock proteins were mostly downregulated upon RPI-1 exposure for 24h (Fig. 4). Again, the analysis of all samples of RPI-1-treated cells without any temporal segregation, revealed the deregulation of a significant fraction ($P<0.001$) of genes involved in the MAP kinase signaling pathway**,** thus confirming the strong impact exerted by the drug on downstream pathways controlling cell proliferation/survival (Tables 1-3 in Supplementary Data).

Validation at the protein level of some of the transcripts modulated upon RPI-1 treatment was performed by Western blot analysis. FGF-R3 downregulation was already detectable after 6h of treatment and appeared preceded by a decrease in tyrosine phosphorylation (Fig. 5A). Inhibition of JAK2 phosphorylation followed similar kinetics, although JAK2 transcript/protein expression was not modulated by drug treatment (data not shown and Fig. 5A). A decrease in BCMA protein levels was evident starting from 15h of RPI-1 treatment (Fig. 5B) whereas Myc downregulation was already detectable at 6h (Fig. 5C). Since Myc is known to suppress the expression of $p27^{Kip1}$ through different mechanisms [30], we also examined the protein levels of this cyclin-dependent kinase inhibitor. RPI-1-induced Myc downregulation was in fact reflected in $p27^{Kip1}$ upregulation at any time point (Fig. 8C). Such an opposite effect of RPI-1 on Myc and $p27^{Kip1}$ expression, together with the modulation of other cell cycle regulators (p21 and CDC25A) and histone family members (Tables 1-3 in Supplementary Data), strongly suggested a cell-cycle arrest of treated cells at the G1/S boundary [31]. Dose-response experiments (Figures 5B and 5C) provided further validation of protein expression modulations in KMS11 cells. Inhibition of JAK2 tyrosine phosphorylation and downregulation of BCMA and Myc, were also

observed in KMS18 cells, thus indicating that these RPI-1 effects are not restricted to the KMS11 myeloma cell line (Supplementary Data, Fig. S2).

3.6. Inhibition of cell growth and Matrigel invasion induced by conditioned medium from mesenchymal stromal cells (MSCs)

The concomitant inhibition of FGF-R3, JAK2/STAT3, and BCMA signaling pathways in RPI-1-treated KMS11 cells suggested a potential ability of the drug to interfere with the tumor cell response to stimuli provided by the BM microenvironment. To explore such issue, we tested the effects of RPI-1 on the MM cells in the presence of culture medium conditioned by BM-derived MSCs (Fig. 6). The conditioned medium significantly increased either cell growth or the cell ability to invade an artificial extracellular matrix such as Matrigel; in both assays, the enhancement was abrogated by RPI-1 treatment (Figures 6A and 6B). Similarly, at the biochemical level, increased STAT3 activation induced by the MSCs' conditioned medium was abrogated (Fig. 6C). Whereas dose-dependent inhibition of KMS11 cell growth was maintained even in the MSC medium, the growth of the MSCs was not significantly affected by the drug (not shown).

4. Discussion

MM is characterized by complex heterogeneous cytogenetic abnormalities [2]. In cooperation with the driving tumorigenic effects of genetic lesions within MM cells, the BM microenvironment provides essential support to the propagation and expansion of malignant clones and promotes drug resistance [8,26,32]. Based on such evidence, concomitant targeting of intrinsically-deregulated and BM microenvironment-sustained proliferation/survival pathways

may offer a new exploitable treatment strategy in MM [8,10,26]. The present study indicates that such a goal may be approached by a single multi-target agent. In fact, the 2-indolinone tyrosine kinase inhibitor RPI-1 was shown to inhibit both FGF-R3, aberrantly expressed in t(4;14)-harboring MM cells, and JAK2, a major effector of IL-6 signaling. Moreover, analysis of GEP in RPI-1-treated cells revealed the downregulation of BCMA, a B-cell-specific receptor of growth factors that regulate growth and survival of MM. Thereby, three crucial signaling pathways, either dependent on oncogene activation or regulated by the BM microenvironment, were abrogated by drug treatment in MM cells.

Sensitivity to RPI-1 was higher in cells expressing an activated FGF-R3. These findings are consistent with previous reports with other FGF-R3 inhibitors indicating a strong dependence of KMS11 and OPM2 cells on constitutive FGF-R3 signaling for proliferation/survival [33-35]. However, the RPI-1 ability to abrogate KMS18 cell growth enhancement provided by aFGF, suggests a potential benefit extended to t(4;14) MM not expressing a constitutively active FGFR3. Our data indicate that the mechanism of FGF-R3 inhibition by RPI-1 may differ from that of other tyrosine kinase inhibitors. Indeed, RPI-1-induced FGF-R3 inactivation was achieved through both kinase inhibition and expression downregulation as detected at both RNA and protein level. This could be a peculiar aspect of the mechanism of receptor tyrosine kinase inactivation by this drug, because similar effects were observed on Ret and Met [15-17]. Although elucidating the molecular bases of such RPI-1 mechanism of action was out of the aim of this study, it is worth noting that JAK2 protein expression, similarly to other cytoplasmic tyrosine kinases such as the Ret/ptcs oncoproteins [13,14] was not modulated by drug treatment, thus suggesting a differential target-dependent modality of tyrosine kinase inactivation.

GEP showed that RPI-1 treatment of KMS11 cells modulated genes recently described as specific components of the FGF-R3 activation pathways such as *SAT-1, ATF3* and *MIP-1α/1β*

[36]. In particular, we observed a concordant modulation at every time point of *SAT-1* and *SRM,* both involved in the cellular polyamine metabolism [37]. The concerted up and downregulation of the catabolic *SAT-1* and the biosynthetic *SRM* enzyme, respectively, is expected to result in a reduction of the cellular polyamine pools, a condition associated with growth inhibition and apoptosis [38]. Indeed, targeting the polyamine pathway may have clinical relevance in anticancer therapy[3]. The upregulation of *ATF3* induced by drug treatment may be relevant in anti-myeloma therapy as ATF3 is known to inhibit IL-6 and IL-12B transcription by altering chromatin structure and restricting access to transcription factors [39]. In addition, RPI-1 led to early downregulation of *MIP-1α* and *MIP-1β ,* two chemokines produced by MM cells and implicated in the pathogenesis of myeloma bone disease [27,28]. Besides its role in development of osteolytic bone destruction, *MIP-1α* might play a pivotal role in the pathogenesis of MM directly affecting cell signaling pathways that mediate growth, survival, and migration in MM cells and promoting adhesive interactions between MM and stromal cells [27]. Consistent with the potential implication of DUSP family in FGF-R3 signaling [36], GEP of RPI-1-treated cells also revealed the upregulation of DUSP10, a negative regulator of the MAP kinase cascade. Noteworthy, RPI-1 treatment downregulated also *SFRS1,* a splicing factor-encoding gene recently described as a proto-oncogene and a potential target for cancer therapy [40].

We show here that, together with FGF-R3, JAK2 is an RPI-1 target in MM cells. The potential therapeutic relevance of JAK2 in the treatment of MM is well recognized and related to its role as an effector of the signaling cascade induced by IL-6, a major growth and anti-apoptotic factor implicated in both autocrine and paracrine MM cell stimulation within the BM milieu [8,12,41]. It has been reported that IL-6 also participate to the regulation of BCMA expression [42], thus the early and stable downregulation of this receptor detected in KMS11 cells after RPI-

1 treatment was conceivably an indirect effect of JAK2/STAT3 pathway inhibition. Accordingly, drug treatment inhibited JAK2 and downregulated BCMA also in KMS18 cells. Several lines of evidence point to BCMA as a potential therapeutic target in MM [43]. It represents indeed a major receptor of the two myeloma cell growth/survival factors, B cell-activating factor (BAFF) and a proliferation-inducing ligand (APRIL), produced by the BM MSCs [29]. A role for BAFF/BCMA signaling has been established in interaction and adhesion of MM cells with BM stromal cells [44]. Moreover, studies in $BCMA^{-/-}$ mice indicate a pivotal role for the receptor in the survival of long-lived BM plasma cells [45] and high levels of BCMA have been found in malignant plasma cells [46].

RPI-1 showed the ability to overcome proliferation and pro-invasive stimuli provided to MM cells by BM-derived MSCs. These findings support that the concomitant inhibition of FGF-R3, JAK2/STAT3 and BCMA signaling pathways may, at least in part, counteract MM cell growth, survival and invasive stimuli sustained by the BM microenvironment. Our in vitro data indicate that the abrogation of growth factor-mediated signaling cascades was reflected in the inhibition of downstream pathways involving ERKs, AKT and STAT3. As a result, a perturbation of cell cycle progression, as suggested by the modulation of cell cycle regulators including Myc, $p27^{Kip1}$, p21 and CDC25A, was associated with caspase-dependent apoptosis. Further analysis of the determinants of RPI-1-induced cell death showed that drug treatment affected two additional proteins implicated in the MM pathobiology, Mcl-1 and survivin, both functioning as key regulators of cell survival [25,47]. Apoptosis was in fact characterized by increased detection of low molecular weight forms of Mcl-1 and downregulation of survivin. The generation of pro-apoptotic peptides by caspase-dependent cleavage of Mcl-1 has been described as an effective mechanism contributing to MM cell apoptosis even in the absence of substantial reduction of full-length Mcl-1 levels [26]. Nonetheless, because these peptides could be observed

even in untreated cells, the expression of alternatively spliced forms of Mcl-1 cannot be ruled out [48]. The decrease in survivin expression, which was not appreciated at RNA level, was likely a consequence of PI3K/AKT pathway inhibition, as previously shown by specific AKT inhibition in the MM cell context [32]. Notably, modulation of Mcl-1 and survivin, as well as AKT, may have therapeutic relevance in this disease [25,47,49].

A number of tyrosine kinase inhibitors targeting FGF-R3 or JAK2 have shown anti-myeloma activity in preclinical studies [33,34,35,41,50] and a few of them are currently being evaluated in phase I/II clinical trials in patients with relapsed or refractory MM[3]. The peculiar FGF-R3/JAK2 targeting profile exhibited by RPI-1 shows the feature to counteract multiple stimuli in MM cells, deriving by either the specific genetic alteration or the BM microenvironment. These findings provide a rationale for the development of treatment strategies resulting in a concomitant inhibition of FGF-R3 and JAK2 kinase signaling. Such therapeutic approaches may have relevance in t(4;14) positive MM which represents the highest risk prognostic variant [3,4] and may potentially contribute to overcoming resistance to conventional therapy.

Acknowledgements

This study was supported in part by Associazione Italiana per la Ricerca sul Cancro to AN and FZ, Ministero della Salute and Alleanza Contro il Cancro. The authors thank the Medicinal Chemistry Department of Cell Therapeutics, Inc., Europe (Bresso, Italy), for the synthesis of RPI-1, Luigia Lombardi for critical review and Laura Zanesi for help in editing the manuscript.

Disclosure of potential conflicts of interest

The authors reported no potential conflicts of interest.

References

[1] Hideshima T, Mitsiades C, Tonon G, Richardson PG, Anderson KC. Understanding multiple myeloma pathogenesis in the bone marrow to identify new therapeutic targets. Nature Rev 2007; 7:585-98.

[2] Chng WJ, Glebov O, Bergsagel PL, Kuehl WM. Genetic events in the pathogenesis of multiple myeloma. Best Pract Res Clin Haematol 2007; 20:571-96.

[3] Richelda R, Ronchetti D, Baldini L, Cro L, Viggiano L, Marzella R, et al. A novel chromosomal translocation t(4; 14)(p16.3; q32) in multiple myeloma involves the fibroblast growth-factor receptor 3 gene. Blood 1997; 90:4062-70.

[4] Todoerti K, Ronchetti D, Agnelli L, Castellani S, Marelli S, Deliliers GL, et al. Transcription repression activity is associated with the type I isoform of the MMSET gene involved in t(4; 14) in multiple myeloma. Br J Haematol 2005; 131:214-8.

[5] Chesi M, Bergsagel PL, Kuehl WM. The enigma of ectopic expression of FGRF3 in multiple myeloma: a critical initiating event or just a target for mutational activation during tumor progression. Curr Opin Hematol 2002; 9:288-293.

[6] Onwuazor ON, Wen XY, Wang DY, Zhuang L, Masih-Khan E, Claudio J, et al. Mutation, SNP, and isoform analysis of fibroblast growth factor receptor 3 (FGFR3) in 150 newly diagnosed multiple myeloma patients. Blood 2003; 102:772-3.

[7] Ronchetti D, Greco A, Compasso S, Colombo G, Dell'Era P, Otsuki T, et al. Deregulated FGFR3 mutants in multiple myeloma cell lines with t(4;14): comparative analysis of Y373C, K650E and the novel G384D mutations. Oncogene 2001; 20:3553-62.

[8] Mitsiades CS, Mitsiades NS, Richardson PG, Munshi NC, Anderson KC. Multiple myeloma: a prototypic disease model for the characterization and therapeutic targeting of interaction between tumor cells and their local microenvironment. J Cell Biochem 2007;

101:950-68.

[9] Van de Donk NWCJ, Lokhorst HM, Bloem AC. Growth factors and antiapoptotic signaling pathways in multiple myeloma. Leukemia 2005; 19:2177-85.

[10] Bommert K, Bargou RC, Stuhmer T. Signalling and survival pathways in multiple myeloma. Eur J Cancer 2006; 42:1574-80.

[11] Yasui H, Hideshima T, Richardson PG, Anderson KC. Novel therapeutic strategies targeting growth factor signaling cascades in multiple myeloma. Br J Haematol 2006; 132:385-97.

[12] Podar K, Chauhan D, Anderson KC. Bone marrow microenvironment and the identification of new targets for myeloma therapy. Leukemia 2008; advanced online publication.

[13] Lanzi C, Cassinelli G, Pensa T, Cassinis M, Gambetta RA, Borrello MG, et al. Inhibition of transforming activity of the ret/ptc1 oncoprotein by a 2-indolinone derivative. Int J Cancer 2000; 85:384-90.

[14] Lanzi C, Cassinelli G, Cuccuru G, Zaffaroni N, Supino R, Vignati S, et al. Inactivation of Ret/Ptc1 oncoprotein and inhibition of papillary thyroid carcinoma cell proliferation by indolinone RPI-1. Cell Mol. Life Sci 2003; 60:1449-59.

[15] Cuccuru G, Lanzi C, Cassinelli G, Pratesi G, Tortoreto M, Petrangolini G, et al. Cellular effects and antitumor activity of RET inhibitor RPI-1 on MEN2A-associated medullary thyroid carcinoma. J Natl Cancer Inst 2004; 96:1006-14.

[16] Petrangolini G, Cuccuru G, Lanzi C, Tortoreto M, Belluco S, Pratesi G, et al. Apoptotic cell death induction and angiogenesis inhibition in large established medullary thyroid carcinoma xenografts by Ret inhibitor RPI-1. Biochem Pharmacol 2006; 72:405-14.

[17] Cassinelli G, Lanzi C, Petrangolini G, Tortoreto M, Pratesi G, Cuccuru G, et al. Inhibition

of c-Met and prevention of spontaneous metastatic spreading by the 2-indolinone RPI-1. Mol Cancer Ther 2006; 5:2388-97.

[18] Cassinelli G, Favini E, Degl'Innocenti D, Salvi A, De Petro G, Pierotti MA, et al. RET/PTC1-driven neoplastic transformation and pro invasive phenotype of human thyrocytes involve Met induction and β-catenin nuclear translocation. Neoplasia 2009; 11:10-21.

[19] Agnelli L, Bicciato S, Mattioli M, Fabris S, Intini D, Verdelli D, et al. Molecular classification of multiple myeloma: a distinct transcriptional profile characterizes patients expressing CCND1 and negative for 14q32 translocations. J Clin Oncol 2005; 23:7296-306.

[20] Mattioli M, Agnelli L, Fabris S, Baldini L, Morabito F, Bicciato S, et al. Gene expression profiling of plasma cell dyscrasias reveals molecular patterns associated with distinct IGH translocations in multiple myeloma. Oncogene 2005; 24:2461-73.

[21] Klein U, Tu Y, Stolovitzky GA, Mattioli M, Cattoretti G, Husson H, et al. Gene expression profiling of B cell chronic lymphocytic leukemia reveals a homogeneous phenotype related to memory B cells. J Exp Med 2001; 194:1625-38.

[22] Schadt EE, Li C, Ellis B, Wong WH. Feature extraction and normalization algorithms for high-density oligonucleotide gene expression array data. J Cell Biochem Suppl 2001; 37:120-5.

[23] Lombardi L, Poretti G, Mattioli M, Fabris S, Agnelli L, Bicciato S, et al. Molecular characterization of human multiple myeloma cell lines by integrative genomics: insights into the biology of the disease. Genes, Chromosomes & Cancer 2007; 46:226-38.

[24] Ishikawa H, Tsuyama N, Liu S, Abroun S, Li F-J, Otsuyama K-i, et al. Accelerated proliferation of myeloma cells by interleukin-6 cooperating with fibroblast growth factor

receptor 3-mediated signals. Oncogene 2005; 24:6328-32.

[25] Romagnoli M, Trichet V, David C, Clement M, Moreau P, Bataille R, et al. Significant impact of survivin on myeloma cell growth. Leukemia 2007; 21:1070-8.

[26] Podar K, Gouill SL, Zhang J, Opferman JT, Zorn E, Tai YT, et al. A pivotal role for Mcl-1 in bortezomib-induced apoptosis. Oncogene 2008; 27:721-31.

[27] Terpos E, Politou M, Viniou N, Rahemtulla A. Significance of macrophage inflammatory protein-1 alpha (MIP-1alpha) in multiple myeloma. Leuk Lymphoma 2005; 46:1699-707.

[28] Hashimoto T, Abe M, Oshima T, et al. Ability of myeloma cells to secrete macrophage inflammatory protein (MIP)-1alpha and MIP-1beta correlates with lytic bone lesions in patients with multiple myeloma. Br J Haematol 2004; 125:38-41.

[29] Novak AJ, Darce JR, Arendt BK, Harder B, Henderson K, Kindsvogel W, et al. Expression of BCMA, TACI, and BAFF-R in multiple myeloma: a mechanism for growth and survival. Blood 2004; 103:689-94.

[30] Keller UB, Old JB, Dorsey FC, Nilsson JA, Nilsson L, MacLean KH, et al. Myc targets Cks1 to provoke the suppression of $p27^{Kip1}$, proliferation and lymphomagenesis. EMBO J 2007; 26:2562-74.

[31] Ewen ME. Where the cell cycle and histones meet. Genes Dev 2000; 14:2265-70.

[32] Hideshima T, Catley L, Raje N, Chauhan D, Podar K, Mitsiades C, et al. Inhibition of Akt induces significant downregulation of surviving and cytotoxicity in human multiple myeloma cells. Br J Haematol 2007; 138:783-91.

[33] Grand EK, Chase AJ, Heath C, Rahemtulla A, Cross NCP. Targeting FGFR3 in multiple myeloma: inhibition of t(4;14)-positive cells by SU5402 and PD173074. Leukemia 2004; 18:962-6.

[34] Trudel S, Li ZH, Wei E, Wiesmann M, Chang H, Chen C, et al. CHIR-258, a novel,

multitargeted tyrosine kinase inhibitor for the potential treatment of t(4;14) multiple myeloma. Blood 2005; 105:2941-8.

[35] Bisping G, Kropff M, Wenning D, Dreyer B, Bessonov S, Hilberg F, et al. Targeting receptor kinases by a novel indolinone derivative in multiple myeloma: abrogation of stroma-derived interleukin-6 secretion and induction of apoptosis in cytogenetically defined subgroups. Blood 2006; 107:2079-89.

[36] Masih-Khan E, Trudel S, Heise C, Li Z, Paterson J, Nadeem V, et al. MIP-1alpha (CCL3) is a downstream target of FGFR3 and RAS-MAPK signaling in multiple myeloma. Blood 2006; 108:3465-71.

[37] Criss WE. A review of polyamines and cancer. Turk J Med Sci 2003; 33:195-205.

[38] Allen WL, McLean EG, Boyer J, McCulla A, Wilson PM, Coyle V, et al. The role of spermidine/spermine N^1-acetyltransferase in determining response to chemotherapeutic agents in colorectal cancer cells. Mol Cancer Ther 2007; 6:128-37.

[39] Gilchrist M, Thorsson V, Li B, Rust AG, Korb M, Roach JC, et al. Systems biology approaches identify ATF3 as a negative regulator of Toll-like receptor 4. Nature 2006; 441:173-8.

[40] Karni R, de Stanchina E, Lowe SW, Sinha R, Mu D, Krainer AR. The gene encoding the splicing factor SF2/ASF is a proto-oncogene Nat Struct Mol Biol. 2007; 14:185-93.

[41] Pedranzini L, Dechow T, Berishaj M, Comenzo R, Zhou P, Azare J, et al. Pyridone 6, a pan-janus-activated kinase inhibitor, induces growth inhibition of multiple myeloma cells. Cancer Res 2006; 66:9714-21.

[42] Yang M, Hase H, Legarda-Addison D, Varughese L, Seed B, Ting AT. B cell maturation antigen, the receptor for a proliferation-inducing ligand and B cell-activating factor of the TNF family, induces antigen presentation in B cells. J Immunol 2005; 175:2814-24.

[43] Ryan MC, Hering M, Peckham D, McDonagh CF, Brown L, Kim KM, et al. Antibody targeting of B-cell maturation antigen on malignant plasma cells. Mol Cancer Ther 2007; 6:3009-18.

[44] Tai Y-T, Li X-F, Breitkreutz I, Song W, Neri P, Catley L, et al. Role of B-cell-activating factor in adhesion and growth of human multiple myeloma cells in the bone marrow microenvironment. Cancer Res 2006; 66:6675-82.

[45] O'Connor BP, Raman VS, Erickson LD, Cook WJ, Weaver LK, Ahonen C, et al. BCMA is essential for the survival of long-lived bone marrow plasma cells. J Exp Med 2004; 199:91-7.

[46] Claudio JO, Masih-Khan E, Tang H, Goncalves J, Voralia M, Li ZH, et al. A molecular compendium of genes expressed in multiple myeloma. Blood 2002; 100:2175-86.

[47] Le Gouill S, Podar K, Harousseau J-L, Anderson KC. Mcl-1 regulation and its role in multiple myeloma. Cell Cycle 2004; 3:107-10.

[48] Gómez-Benito M, Martinez-Lorenzo MJ, Anel A, Marzo I, Naval J. Membrane expression of DR4, DR5 and caspase-8 levels, but not Mcl-1, determine sensitivity of human myeloma cells to Apo2L/TRAIL. Exp Cell Res 2007; 313:2378-88.

[49] Harvey RD, Lonial S. PI3 kinase/AKT pathway as a therapeutic target in multiple myeloma. Future Oncol 2007; 3:639-47.

[50] Chen J, Lee BH, Williams IR, Kutok JL, Mitsiades CS, Duclos N, et al. FGFR3 as a therapeutic target of the small molecule inhibitor PKC412 in hematopoietic malignancies. Oncogene 2005; 24:8259-67.

Web references

[1] http://david.niaid.nih.gov/david/version2/index.htm

[2] https://www.affymetrix.com/analysis/netaffx/

[3] http://www.clinicaltrials.gov

Figure legends

Figure 1. Effect of RPI-1 treatment on cell viability of representative HMCLs detected by Trypan blue dye exclusion assay. **A,** Mean dose-response curves obtained in at least two independent experiments (performed in duplicate) with KMS20, KMS11 and OPM2 cells incubated with the drug for 72h. Each point represents the mean percentage of the control viable cell number value**. B,** Time-course of growth inhibitory effect on KMS18 and KMS11 cell lines. Solvent or RPI-1 (25 μM) were added to cell cultures the day after splitting (arrow). Viable cells were counted every day. Data (mean ± SD) from one experiment representative of three is shown. **C,** Inhibition of cell growth enhancement induced by aFGF. KMS18 cells were treated with solvent (-) or 25 μM RPI-1 (+) in the absence (-) or presence (+) of aFGF/heparin as indicated. Viable cells were counted after 72h. Bars represent mean values ± SD. One experiment representative of three is shown. (*, $P < 0.0005$).

Figure 2. Inhibition of FGF-R3- and JAK2-mediated signaling by RPI-1. **A,** Inhibition of FGF-R3^{Y373C} constitutive activation and expression in NIH3T3 transfectants (A6-KMS11). Cells were treated with the indicated concentrations of the drug for 72h. Western blot analysis with anti-pan-phosphotyrosine (pTyr) or anti-FGF-R3 antibodies was performed on FGF-R3 immunoprecipitates (IP) or whole cell lysates (WCL) as indicated. In the lower panel, a cell lysate from NIH-3T3 parent cells was run in parallel as a negative control for FGF-R3 expression. **B,** Inhibition of endogenous FGF-R3^{Y373C} tyrosine phosphorylation and expression in the HMCL KMS11. Cells were treated with RPI-1 (3, 10 and 30 μM) for 24h and processed for Western blot analysis as in (A). **C,** Inhibition of aFGF-induced signaling in KMS11 cells. Serum

starved cells were incubated in the presence of vehicle (-) or RPI-1 (10 or 30 μM) for 6h. Cells were then left untreated (-) or stimulated with aFGF/heparin (+) for 5 min as indicated. The activated status of receptor and downstream pathways was analyzed in cell lysates by Western blotting with phospho-specific antibodies recognizing activated FGF-R3, ERKs, AKT and STAT3. **D,** Inhibition of JAK2/STAT3 activation in KMS11 cells. Serum starved cells were treated with the indicated concentrations of the drug for 24h. Cell lysates were analyzed by Western blotting with phospho-specific antibodies recognizing activated JAK2 or STAT3. In (C) and (D), each blot was stripped and reprobed with the respective anti-protein antibodies. Protein loading is shown by actin.

Figure 3. Apoptosis induction by RPI-1 treatment in KMS11 cells. Cells were incubated in the presence of solvent (control) or RPI-1 (10, 20, 30 and 60 μM), for 72h. **A,** TUNEL assay analyzed by FACS. A representative dose-response experiment is shown together with quantitative data obtained in three independent experiments (panel right bottom). **B,** Modulation of anti-apoptotic factors and caspase activation. Cell lysates were analyzed by Western blotting to detect activating phosphorylations of AKT and STAT3, expression of Bcl-X_L, Mcl-1 and survivin, and cleavage of caspases (9, 8 and 3) and PARP. Blots anti-pAKT and anti-pSTAT3 were stripped and reprobed with the respective anti-protein antibodies. Anti-tubulin blot shows protein loading. Quantitative data reported in **A** (panel right bottom) represent mean values of cell death induced by drug treatment both in **A** and **B**. Histograms represent mean percentages of apoptotic cells ± SD.

Figure 4. Supervised gene expression analysis comparing samples from triplicates of KMS11 cells treated with 30 μM RPI-1 (T) or vehicle (C) for 24h. The expression levels of the identified

genes in cells treated with RPI-1 for 6h and 15h are shown on the right side of the figure. Full support and δ-value of 0.02 was used in the analysis. Genes differentially expressed in drug-treated vs control cells are grouped according to their functional categories and ranked within each category according to their Zg score. Zg scores and fold changes (FC) are expressed using the control group as baseline. The color scale bar represents the relative gene expression changes normalized by the standard deviation.

Figure 5. Modulation of selected gene products in KMS11 cells treated with RPI-1. Whole cell lysates were analyzed by Western blotting. In time-course experiments, cells were treated with solvent (-) or 30 μM RPI-1 (+) for the indicated times. In the dose-response experiments shown in B, and C, cells were treated with solvent (-) or increasing drug concentrations (3, 10, 30, 60 μM) for 24h. **A,** Inhibition of FGF-R3 and JAK2 activation evidenced as abrogation of tyrosine phosphorylation (pFGF-R and pJAK2), and downregulation of FGF-R3 protein expression. **B,** Downregulation of BCMA expression. **C,** Downregulation of Myc and upregulation of p27 expression. Tubulin or actin blots are shown as controls for protein loading.

Figure 6. Abrogation of the stimulating effects of conditioned medium from mesenchymal stromal cells (MSCs) on cell growth and invasive properties of KMS11 cells by RPI-1 treatment. **A,** Cell viability assay. KMS11 cells cultured in the proper (MM) or MSCs-derived conditioned medium were treated with solvent (-) or the indicated concentrations of the drug for 72 h. Cell viability was assessed by MTT colorimetric assay and expressed as optical density (OD) at 550 nm. **B,** Invasion assay. Cells were exposed to 20 μM RPI-1 for 24 h and then subjected to Matrigel invasion assay in the presence of the proper (MM) or MSCs-derived medium. Invading

cells were colored and counted under microscope. Bars represent mean values ± SD. **C**, Inhibition of STAT3 activation. Cell lysates from cells treated as in **B**, were subjected to Western blotting and probed with anti-phospho-STAT3 antibody (pSTAT3). The blot was then stripped and reprobed with anti-STAT3 antibody. Anti-actin blot shows protein loading. Data shown are representative of three independent experiments. (*, $P < 0.0005$).

Table 1. Antiproliferative effect of RPI-1 on human MM cell lines (HMCLs)

HMCL*	t(4;14)	FGFR3 status	RPI-1 (IC_{50}, μM)
OPM2	+	K650E (kinase domain, activating)	4.9 ± 0.1 (n = 2)
KMS11	+	Y373C (transmembrane, activating)	10.8 ± 0.8 (n = 3)
KMS18	+	G384D (transmembrane, not transforming)	36.3 ± 9.9 (n = 5)
KMS28	+	wt	27.6 ± 8.6 (n = 4)
KMS20	-	-	> 45 (n = 4)
JJN3	-	-	32.4 ± 6.8 (n = 3)

*KMS11 and JJN3 cell lines harbor the t(14;16) translocation. OPM2 has a translocation involving MAFB gene at chromosome 20 together with an unidentified partner chromosome. KMS20 is negative for any known chromosome translocation (23).

Supplementary data.

Supervised analysis of KMS11 RPI-1-treated *versus* KMS11 untreated cells.

Table 1a Twenty-six up-regulated probes in KMS11 upon 6h RPI-1-treatment, ordered by gene name.

Probe ID	GENE	NAME	Biological Process	Zscore	FC
207623_at	ABCF2	ATP-binding cassette, sub-family F (GCN20), member 2	transport	10.186	8.8976898
207571_x_at	C1orf38	chromosome 1 open reading frame 38	cell adhesion	16.365	4.1309401
210785_s_at	C1orf38	chromosome 1 open reading frame 38	cell adhesion	7.812	3.7808393
210689_at	CLDN14	claudin 14	protein complex assembly	40.369	7.3953488
204724_s_at	COL9A3	collagen, type IX, alpha 3	phosphate transport	19.351	7.6466083
203947_at	CSTF3	cleavage stimulation factor, 3' pre-RNA, subunit 3, 77kDa	mRNA processing	5.695	3.2016276
219233_s_at	GSDML	gasdermin-like	---	9.505	4.3386628
208579_x_at	H2BFS / HIST1H2BK	H2B histone family, member S / histone cluster 1, H2bk	nucleosome assembly	8.257	4.1768187
215071_s_at	HIST1H2AC	histone cluster 1, H2ac	nucleosome assembly	10.437	6.0092814
209806_at	HIST1H2BK	histone cluster 1, H2bk	nucleosome assembly	9.692	2.8170327
214522_x_at	HIST1H3D	histone cluster 1, H3d	nucleosome assembly	5.943	13.805085
206110_at	HIST1H3H	histone cluster 1, H3h	nucleosome assembly	9.421	5.5302083
214290_s_at	HIST2H2AA3 / HIST2H2AA4	histone cluster 2, H2aa3 / histone cluster 2, H2aa4	nucleosome assembly	9.957	2.4075915
218280_x_at	HIST2H2AA3 / HIST2H2AA4	histone cluster 2, H2aa3 / histone cluster 2, H2aa4	nucleosome assembly	5.405	3.1270189
213776_at	LOC157562	hypothetical protein LOC157562	---	7.087	5.5628141
213225_at	PPM1B	protein phosphatase 1B (formerly 2C), magnesium-dependent, beta isoform	protein amino acid dephosphorylation	4.272	4.6496815
200749_at	RAN	RAN, member RAS oncogene family	regulation of progression through cell cycle	4.917	3.2060944
202388_at	RGS2	regulator of G-protein signalling 2, 24kDa	cell cycle	25.048	5.1233576
209070_s_at	RGS5	regulator of G-protein signalling 5	regulation of G-protein coupled receptor protein signaling pathway	3.675	6.061828
209071_s_at	RGS5	regulator of G-protein signalling 5	regulation of G-protein coupled receptor protein signaling pathway	3.435	6.0876068
212019_at	RSL1D1	ribosomal L1 domain containing 1	translation	6.581	4.9563427

213750_at	RSL1D1	ribosomal L1 domain containing 1	translation	30.956	4.6814048
203455_s_at	SAT1	spermidine/spermine N1-acetyltransferase 1	metabolic process	8.988	6.1119048
210592_s_at	SAT1	spermidine/spermine N1-acetyltransferase 1	metabolic process	17.694	8.0817518
213988_s_at	SAT1	spermidine/spermine N1-acetyltransferase 1	metabolic process	17.814	22.983871
208078_s_at	SNF1LK	SNF1-like kinase	negative regulation of transcription from RNA polymerase II promoter	5.925	2.7429859

Table 1b Thirty-two down-regulated probes in KMS11 upon 6h RPI-1-treatment, ordered by gene name.

Probe ID	GENE	NAME	Biological Process	Zscore	FC
40472_at	AGPAT7	1-acylglycerol-3-phosphate O-acyltransferase 7 (lysophosphatidic acid acyltransferase, eta)	metabolic process	-8.254	-5.815047022
202760_s_at	AKAP2	A kinase (PRKA) anchor protein 2	regulation of cell shape	-8.947	-4.634046053
201084_s_at	BCLAF1	BCL2-associated transcription factor 1	regulation of transcription	-11.226	-2.802586207
201101_s_at	BCLAF1	BCL2-associated transcription factor 1	regulation of transcription	-8.748	-8.460588794
205114_s_at	CCL3/ MIP-1α	chemokine (C-C motif) ligand 3	cell-cell signaling	-8.326	-15.40503247
204103_at	CCL4/ MIP-1β	chemokine (C-C motif) ligand 4	cell-cell signaling	-4.893	-18.88023952
204118_at	CD48	CD48 molecule	defense response	-19.868	-3.601732435
202613_at	CTPS	CTP synthase	nucleic acid metabolic process	-10.976	-3.289522919
210137_s_at	DCTD	dCMP deaminase	nucleic acid metabolic process	-5.528	-3.030553865
212728_at	DLG3	discs, large homolog 3 (neuroendocrine-dlg, Drosophila)	regulation of cell proliferation	-4.286	-5.608200456
203638_s_at	FGFR2	fibroblast growth factor receptor 2	protein amino acid phosphorylation; cell growth	-4.72	-4.882352941
215967_s_at	LY9	lymphocyte antigen 9	cell adhesion	-18.782	-16.10240964
210017_at	MALT1	mucosa associated lymphoid tissue lymphoma translocation gene 1	positive regulation of T cell cytokine production	-5.145	-4.302302302
205447_s_at	MAP3K12	mitogen-activated protein kinase kinase kinase 12	JNK cascade	-12.777	-7.346774194
200796_s_at	MCL1	myeloid cell leukemia sequence 1 (BCL2-related)	regulation of apoptosis	-3.78	-3.70783848
202431_s_at	MYC	v-myc myelocytomatosis viral oncogene homolog (avian)	regulation of cell proliferation	-5.559	-2.614602835
222206_s_at	NCLN	nicalin homolog (zebrafish)	protein processing	-3.26	-4.836400818
209062_x_at	NCOA3	nuclear receptor coactivator 3	regulation of transcription,	-6.416	-6.938080495
203823_at	RGS3	regulator of G-protein signalling 3	negative regulation of signal transduction	-63.427	-16.24761905
216392_s_at	SEC23IP	SEC23 interacting protein	intracellular protein transport	-8.067	-3.89797136
208863_s_at	SFRS1	splicing factor, arginine/serine-rich 1 (splicing factor 2, alternate splicing factor)	mRNA processing	-13.795	-3.635181383
200754_x_at	SFRS2	splicing factor, arginine/serine-rich 2	mRNA processing	-3.142	-2.358962421
214882_s_at	SFRS2	splicing factor, arginine/serine-rich 2	mRNA processing	-4.696	-2.673421819

202899_s_at	SFRS3	splicing factor, arginine/serine-rich 3	mRNA processing	-21.044	-3.214740252
208672_s_at	SFRS3	splicing factor, arginine/serine-rich 3	mRNA processing	-9.737	-3.032237266
214141_x_at	SFRS7	splicing factor, arginine/serine-rich 7, 35kDa	mRNA processing	-11.13	-2.635012715
206641_at	TNFRSF17/ BCMA	tumor necrosis factor receptor superfamily, member 17	signal transduction; cell proliferation	-9.737	-8.782380952
217853_at	TNS3	tensin 3	intracellular signaling cascade	-6.888	-2.995089442
213888_s_at	TRAF3IP3	TRAF3 interacting protein 3	---	-9.883	-3.752346194
209013_x_at	TRIO	triple functional domain (PTPRF interacting)	protein amino acid phosphorylation	-3.818	-5.736363636
218245_at	TSKU	tsukushin	---	-21.391	-6.632727273
202864_s_at	SP100	SP100 nuclear antigen	regulation of transcription, DNA-dependent /// regulation of transcription, DNA-dependent	-11.799	-10.65128205

Table 2a Twenty-four up-regulated probes in KMS11 upon 15h RPI-1-treatment, ordered by gene name.

Probe ID	GENE	NAME	Biological Process	Zscore	FC
202284_s_at	CDKN1A	cyclin-dependent kinase inhibitor 1A (p21, Cip1)	regulation of progression through cell cycle	34.931	7.534413
212227_x_at	EIF1	eukaryotic translation initiation factor 1	translational initiation	6.29	1.9578982
204805_s_at	H1FX	H1 histone family, member X	nucleosome assembly	2.638	2.4686474
208579_x_at	H2BFS/ HIST1H2BK	H2B histone family, member S / histone cluster 1, H2bk	nucleosome assembly	4.448	3.1218202
209398_at	HIST1H1C	histone cluster 1, H1c	nucleosome assembly	3.163	2.5475938
215071_s_at	HIST1H2AC	histone cluster 1, H2ac	nucleosome assembly	5.702	4.8790942
214469_at	HIST1H2AE	histone cluster 1, H2ae	nucleosome assembly	3.045	5.6865672
209806_at	HIST1H2BK	H2B histone family, member S / histone cluster 1, H2bk	nucleosome assembly	8.498	2.4928358
214472_at	HIST1H3D	histone cluster 1, H3d	nucleosome assembly	5.709	5.0259865
208496_x_at	HIST1H3G	histone cluster 1, H3g	nucleosome assembly	21.75	25.422764
206110_at	HIST1H3H	histone cluster 1, H3h	nucleosome assembly	9.351	6.0917793
214290_s_at	HIST2H2AA3 / HIST2H2AA4	histone cluster 2, H2aa3 / histone cluster 2, H2aa4	nucleosome assembly	9.215	3.7411356
218280_x_at	HIST2H2AA3 / HIST2H2AA4	histone cluster 2, H2aa3 / histone cluster 2, H2aa4	nucleosome assembly	7.636	4.9598617
200800_s_at	HSPA1A / HSPA1B	heat shock 70kDa protein 1A / heat shock 70kDa protein 1B	mRNA catabolic process	3.834	5.115903
202581_at	HSPA1B	heat shock 70kDa protein 1A / heat shock 70kDa protein 1B	mRNA catabolic process	5.383	4.8661267
117_at	HSPA6	heat shock 70kDa protein 6 (HSP70B')	response to unfolded protein	3.667	11.769097
213418_at	HSPA6	heat shock 70kDa protein 6 (HSP70B')	response to unfolded protein	14.81	29.241055
203752_s_at	JUND	jun D proto-oncogene	regulation of transcription	5.955	2.2876192
37028_at	PPP1R15A	protein phosphatase 1, regulatory (inhibitor) subunit 15A	apoptosis	4.613	3.2170997
202388_at	RGS2	regulator of G-protein signalling 2, 24kDa	cell cycle	3.926	2.9416775
209070_s_at	RGS5	regulator of G-protein signalling 5	regulation of G-protein coupled receptor protein signaling pathway	5.374	6.380805
203455_s_at	SAT1	spermidine/spermine N1-acetyltransferase 1	metabolic process	7.052	5.8085774
210592_s_at	SAT1	spermidine/spermine N1-acetyltransferase 1	metabolic process	17.427	7.6462054
213988_s_at	SAT1	spermidine/spermine N1-acetyltransferase 1	metabolic process	21.964	25.180645

Table 2b Twenty down-regulated probes in KMS11 upon 15h RPI-1-treatment, ordered by gene name.

Probe ID	GENE	NAME	Biological Process	Zscore	FC
214358_at	ACACA	acetyl-Coenzyme A carboxylase alpha	metabolic process	-3.436	-5.6089552
209442_x_at	ANK3	ankyrin 3, node of Ranvier (ankyrin G)	protein targeting	-4.27	-3.5157164
206185_at	CRYBB1	crystallin, beta B1	visual perception	-7.988	-4.2361574
219328_at	DDX31	DEAD (Asp-Glu-Ala-Asp) box polypeptide 31	---	-2.614	-4.4198251
218858_at	DEPDC6	DEP domain containing 6	intracellular signaling cascade	-9.712	-3.065756
201478_s_at	DKC1	dyskeratosis congenita 1, dyskerin	cell proliferation	-2.895	-3.575391
216212_s_at	DKC1	dyskeratosis congenita 1, dyskerin	cell proliferation	-4.984	-10.615213
202345_s_at	FABP5	fatty acid binding protein 5 (psoriasis-associated)	lipid metabolic process	-5.756	-2.9379077
204379_s_at	FGFR3	fibroblast growth factor receptor 3 (achondroplasia, thanatophoric dwarfism)	MAPKKK cascade	-6.977	-1.8886028
214011_s_at	HSPC111	hypothetical protein HSPC111	---	-4.307	-3.6959191
203931_s_at	MRPL12	mitochondrial ribosomal protein L12	translation	-2.904	-2.6991798
202431_s_at	MYC	v-myc myelocytomatosis viral oncogene homolog (avian)	regulation of cell proliferation	-6.505	-3.564178
217356_s_at	PGK1	phosphoglycerate kinase 1	glycolysis	-2.91	-2.3751648
205267_at	POU2AF1	POU domain, class 2, associating factor 1	transcription	-12.326	-2.8488287
218758_s_at	RRP1	ribosomal RNA processing 1 homolog (S. cerevisiae)	rRNA processing	-3.647	-6.4540682
216913_s_at	RRP12	ribosomal RNA processing 12 homolog (S. cerevisiae)	---	-7.513	-10.261146
214141_x_at	SFRS7	splicing factor, arginine/serine-rich 7, 35kDa	mRNA processing	-4.217	-4.0526149
201563_at	SORD	sorbitol dehydrogenase	sorbitol metabolic process	-16.606	-5.0759429
206641_at	TNFRSF17/ BCMA	tumor necrosis factor receptor superfamily, member 17	cell proliferation	-10.678	-8.1686678
209825_s_at	UCK2	uridine-cytidine kinase 2	biosynthetic process	-7.546	-3.53289

Table 3a Thirty-three up-regulated probes in KMS11 upon 24h RPI-1-treatment, ordered by gene name.

Probe ID	GENE	NAME	Biological Process	Zscore	FC
202672_s_at	ATF3	activating transcription factor 3	regulation of transcription	8.525	5.1128641
207571_x_at	C1orf38	chromosome 1 open reading frame 38	cell adhesion	10.231	3.1183007
210785_s_at	C1orf38	chromosome 1 open reading frame 39	cell adhesion	5.492	3.1126835
213348_at	CDKN1C	cyclin-dependent kinase inhibitor 1C (p57, Kip2)	regulation of progression through cell cycle	8.117	4.3138486
216894_x_at	CDKN1C	cyclin-dependent kinase inhibitor 1C (p57, Kip2)	regulation of progression through cell cycle	6.458	4.5855327
219534_x_at	CDKN1C	cyclin-dependent kinase inhibitor 1C (p57, Kip2)	regulation of progression through cell cycle	6.017	3.8604513
219640_at	CLDN15	claudin 15	calcium-independent cell-cell adhesion	2.992	4.5110132
215501_s_at	DUSP10	dual specificity phosphatase 10	protein amino acid dephosphorylation; JNK cascade	2.94	4.2466539
221563_at	DUSP10	dual specificity phosphatase 10	protein amino acid dephosphorylation; JNK cascade	7.978	5.7436233
212227_x_at	EIF1	eukaryotic translation initiation factor 1	translational initiation	2.567	1.7629325
219233_s_at	GSDML	gasdermin-like	---	5.451	4.0514626
215071_s_at	HIST1H2AC	histone cluster 1, H2ac	nucleosome assembly	22.386	4.4343735
214472_at	HIST1H3D	histone cluster 1, H3d	nucleosome assembly	11.537	4.9131915
214522_x_at	HIST1H3D	histone cluster 1, H3d	nucleosome assembly	7.022	4.6964006
208496_x_at	HIST1H3G	histone cluster 1, H3g	nucleosome assembly	4.428	6.1402062
206110_at	HIST1H3H	histone cluster 1, H3h	nucleosome assembly	11.196	4.6453523
214290_s_at	HIST2H2AA3 / HIST2H2AA4	histone cluster 2, H2aa3 / histone cluster 2, H2aa4	nucleosome assembly	7.84	2.5602309
218280_x_at	HIST2H2AA3 / HIST2H2AA4	histone cluster 2, H2aa3 / histone cluster 2, H2aa4	nucleosome assembly	8.251	3.2712434
201464_x_at	JUN	jun oncogene	regulation of progression through cell cycle	3.027	3.3020167
203751_x_at	JUND	jun D proto-oncogene	regulation of transcription	4.487	3.6338656
203752_s_at	JUND	jun D proto-oncogene	regulation of transcription	13.193	2.5481349
221841_s_at	KLF4	Kruppel-like factor 4 (gut)	regulation of transcription	7.638	4.8784029
201669_s_at	MARCKS	myristoylated alanine-rich protein kinase C substrate	cell motility	6.717	3.6042097
37028_at	PPP1R15A	protein phosphatase 1, regulatory (inhibitor) subunit 15A	apoptosis	7.837	3.945816
202988_s_at	RGS1	regulator of G-protein signalling 1	signal transduction	4.321	5.0074513
216834_at	RGS1	regulator of G-protein signalling 1	signal transduction	3.36	2.4548041
202388_at	RGS2	regulator of G-protein signalling 2, 24kDa	cell cycle	6.536	3.0752566

203455_s_at	SAT1	spermidine/spermine N1-acetyltransferase 1	metabolic process	6.718	5.1566265
210592_s_at	SAT1	spermidine/spermine N1-acetyltransferase 1	metabolic process	10.694	5.9428571
213988_s_at	SAT1	spermidine/spermine N1-acetyltransferase 1	metabolic process	16.284	20.706522
201471_s_at	SQSTM1	sequestosome 1	ubiquitin-dependent protein catabolic process; apoptosis	7.247	2.3460443
213112_s_at	SQSTM1	sequestosome 1	ubiquitin-dependent protein catabolic process; apoptosis	9.227	3.2893626
209197_at	SYT11	synaptotagmin XI	transport	9.059	3.9906351

Table 3b Fifty-nine down-regulated probes in KMS11 upon 24h RPI-1-treatment, ordered by gene name.

Probe ID	GENE	NAME	Biological Process	Zscore	FC
214687_x_at	ALDOA	aldolase A, fructose-bisphosphate	metabolic process	-12.88	-2.0994035
201101_s_at	BCLAF1	BCL2-associated transcription factor 1	regulation of transcription	-4.548	-3.9077748
205780_at	BIK	BCL2-interacting killer (apoptosis-inducing)	induction of apoptosis	-13.631	-13.623077
217809_at	BZW2	basic leucine zipper and W2 domains 2	regulation of translational initiation	-16.114	-3.055681
221777_at	C12orf52	chromosome 12 open reading frame 52	---	-4.938	-6.7686275
204695_at	CDC25A	cell division cycle 25 homolog A (S. pombe)	regulation of progression through cell cycle	-2.973	-4.7608696
206533_at	CHRNA5	cholinergic receptor, nicotinic, alpha 5	transport	-25.569	-3.5083144
206185_at	CRYBB1	crystallin, beta B1	visual perception	-8	-11.345345
202937_x_at	CTA-126B4.3	CGI-96 protein	---	-2.536	-3.9650986
219328_at	DDX31	DEAD (Asp-Glu-Ala-Asp) box polypeptide 31	---	-2.402	-4.0957746
201478_s_at	DKC1	dyskeratosis congenita 1, dyskerin	regulation of progression through cell cycle	-7.49	-3.6414863
216212_s_at	DKC1	dyskeratosis congenita 1, dyskerin	regulation of progression through cell cycle	-3.6	-6.8414443
200647_x_at	EIF3S8	eukaryotic translation initiation factor 3, subunit 8, 110kDa	translational initiation	-6.229	-2.810933
211787_s_at	EIF4A1	eukaryotic translation initiation factor 4A, isoform 1	translation	-11.09	-2.5325046
218695_at	EXOSC4	exosome component 4	RNA processing	-2.599	-3.8507653
202345_s_at	FABP5 /	fatty acid binding protein 5 (psoriasis-associated)	lipid metabolic process	-10.141	-4.9094409
204380_s_at	FGFR3	fibroblast growth factor receptor 3	MAPKKK cascade; skeletal development	-14.746	-4.1766544
219271_at	GALNT14	UDP-N-acetyl-alpha-D-galactosamine:polypeptide N-acetylgalactosaminyltransferase 14 (GalNAc-T14)	---	-4.676	-9.4342857
208308_s_at	GPI	glucose phosphate isomerase	carbohydrate metabolic process	-13.454	-2.3725146
200598_s_at	HSP90B1	heat shock protein 90kDa beta (Grp94), member 1	protein folding	-8.318	-2.9437294
216449_x_at	HSP90B1	heat shock protein 90kDa beta (Grp94), member 1	protein folding	-3.614	-5.6564311
208687_x_at	HSPA8	heat shock 70kDa protein 8	protein folding	-9.192	-2.1817546
210338_s_at	HSPA8	heat shock 70kDa protein 8	protein folding	-6.38	-2.3531494
200806_s_at	HSPD1	heat shock 60kDa protein 1 (chaperonin)	protein folding	-13.021	-2.6769356
205133_s_at	HSPE1	heat shock 10kDa protein 1 (chaperonin 10)	protein folding	-5.967	-2.9735466

204744_s_at	IARS	isoleucyl-tRNA synthetase	translation	-13.347	-2.2747016
205902_at	KCNN3	potassium intermediate/small conductance calcium-activated channel, subfamily N, member 3	transport	-38.442	-11.700565
212396_s_at	KIAA0090	KIAA0090		-5.361	-4.0614925
210153_s_at	ME2	malic enzyme 2, NAD(+)-dependent, mitochondrial	malate metabolic process	-9.247	-3.0939496
218664_at	MECR	mitochondrial trans-2-enoyl-CoA reductase	fatty acid metabolic process	-4.16	-4.4507227
221286_s_at	MGC29506	hypothetical protein MGC29506	---	-16.293	-4.7685857
202431_s_at	MYC	v-myc myelocytomatosis viral oncogene homolog (avian)	regulation of cell proliferation	-9.337	-3.8867842
222206_s_at	NCLN	nicalin homolog (zebrafish)	protein processing	-48.216	-16.824324
209062_x_at	NCOA3	nuclear receptor coactivator 3	regulation of transcription	-6.077	-5.0058366
201577_at	NME1	non-metastatic cells 1, protein (NM23A) expressed in	GTP biosynthetic process; regulation of apoptosis	-11.056	-2.7143663
221923_s_at	NPM1	nucleophosmin (nucleolar phosphoprotein B23, numatrin)	intracellular protein transport ; centrosome cycle	-16.131	-2.8534306
201013_s_at	PAICS	phosphoribosylaminoimidazole carboxylase, phosphoribosylaminoimidazole succinocarboxamide synthetase	purine nucleotide biosynthetic process	-13.995	-2.7359484
201014_s_at	PAICS	phosphoribosylaminoimidazole carboxylase, phosphoribosylaminoimidazole succinocarboxamide synthetase	purine nucleotide biosynthetic process	-10.937	-4.2608932
201481_s_at	PYGB	phosphorylase, glycogen; brain	carbohydrate metabolic process	-3.423	-5.5689046
213205_s_at	RAD54L2	RAD54-like 2 (S. cerevisiae)	---	-6.091	-4.7007874
202483_s_at	RANBP1	RAN binding protein 1	spindle organization and biogenesis	-8.356	-2.800464
211955_at	RANBP5	RAN binding protein 5	protein transport	-7.299	-3.7969231
216360_x_at	RRP12	ribosomal RNA processing 12 homolog (S. cerevisiae)		-2.808	-4.2506297
216913_s_at	RRP12	ribosomal RNA processing 12 homolog (S. cerevisiae)		-3.143	-7.419214
204133_at	RRP9	RRP9, small subunit (SSU) processome component, homolog (yeast)	rRNA processing	-9.295	-10.423729
211162_x_at	SCD	stearoyl-CoA desaturase (delta-9-desaturase)	lipid metabolic process	-6.662	-15.764516
211708_s_at	SCD	stearoyl-CoA desaturase (delta-9-desaturase)	lipid metabolic process	-7.944	-5.8237965
208863_s_at	SFRS1	splicing factor, arginine/serine-rich 1 (splicing factor 2, alternate splicing factor)	mRNA processing	-7.147	-3.8212545
200754_x_at	SFRS2	splicing factor, arginine/serine-rich 2	mRNA processing	-4.359	-2.202939

214882_s_at	SFRS2	splicing factor, arginine/serine-rich 2	mRNA processing	-10.561	-2.560161
202899_s_at	SFRS3	splicing factor, arginine/serine-rich 3	mRNA processing	-7.668	-2.7572276
214141_x_at	SFRS7	splicing factor, arginine/serine-rich 7, 35kDa	mRNA processing	-13.206	-3.8248301
203832_at	SNRPF	small nuclear ribonucleoprotein polypeptide F	mRNA processing	-3.581	-2.7466158
201563_at	SORD	sorbitol dehydrogenase	sorbitol metabolic process	-18.386	-5.161442
201516_at	SRM	spermidine synthase	spermidine biosynthetic process	-10.331	-4.0510949
220789_s_at	TBRG4	transforming growth factor beta regulator 4	apoptosis	-4.594	-5.8757396
204281_at	TEAD4	TEA domain family member 4	regulation of transcription	-6.915	-5.9674419
206641_at	TNFRSF17/ BCMA	tumor necrosis factor receptor superfamily, member 17	cell proliferation	-18.124	-8.7394705
209825_s_at	UCK2	uridine-cytidine kinase 2	biosynthetic process	-7.231	-4.1626173

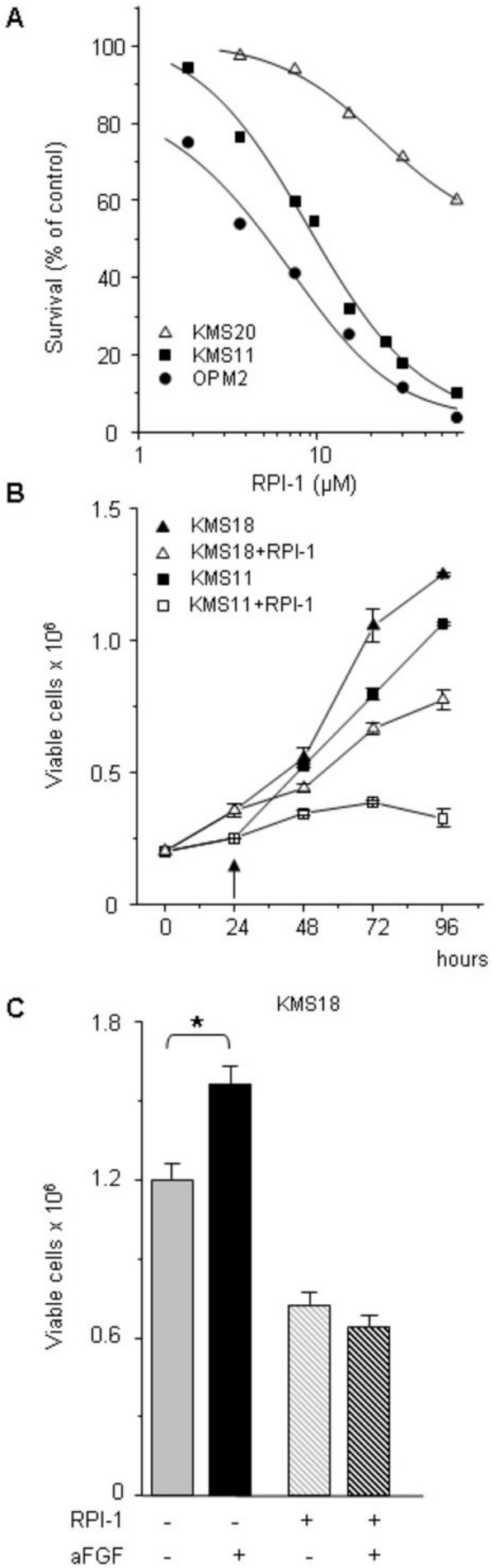
A
Survival (% of control)
100
80
60
40
20
0
KMS20
KMS11
OPM2
1
10
RPI-1 (μM)
B
Viable cells x 10⁶
1.5
1.0
0.5
0
KMS18
KMS18+RPI-1
KMS11
KMS11+RPI-1
0
24
48
72
96
hours
C
KMS18
Viable cells x 10⁶
1.8
1.2
0.6
0
*
RPI-1 - - + +
aFGF - + - +

Fig. 1

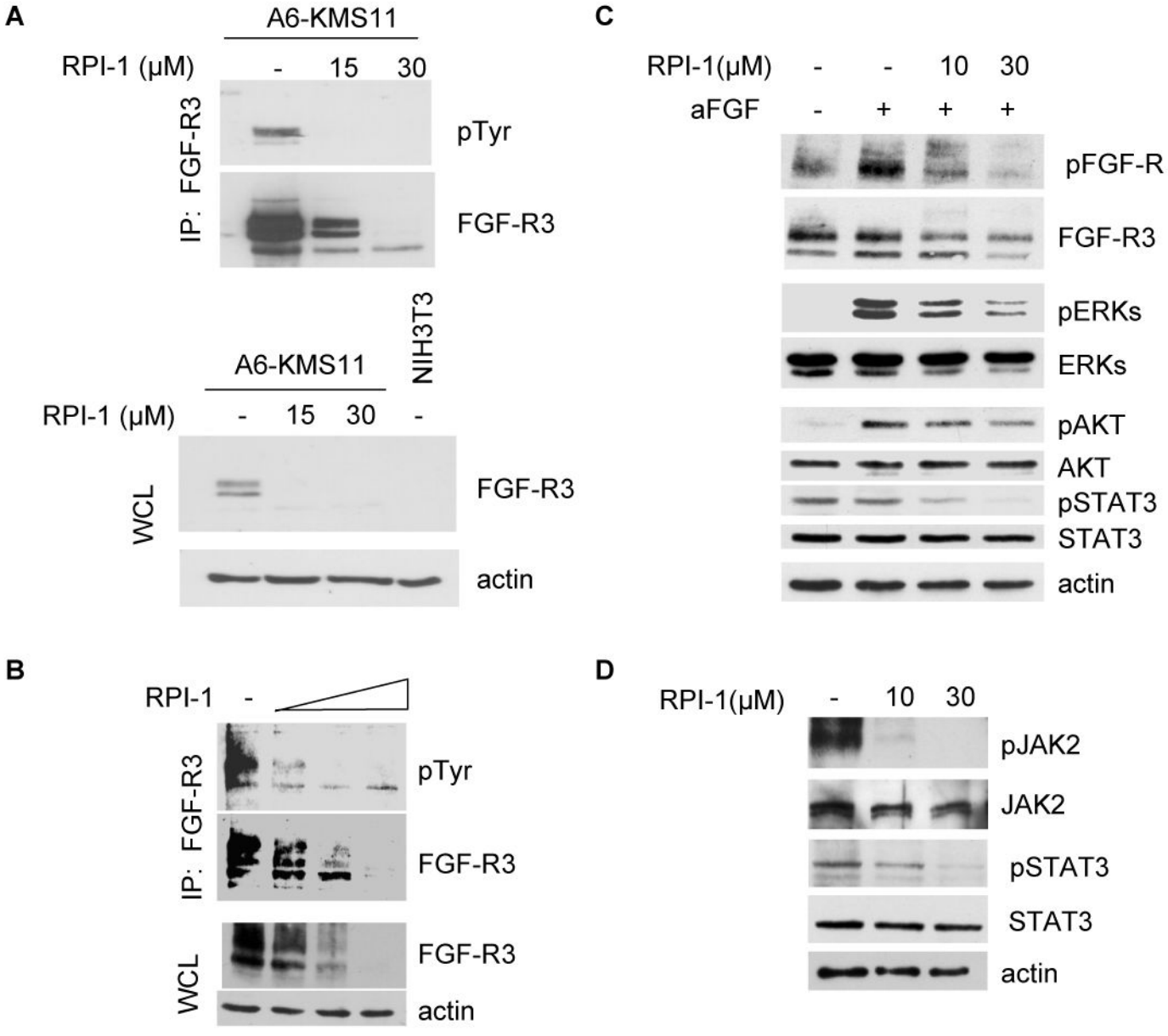
A
A6-KMS11
RPI-1 (μM) - 15 30
IP: FGF-R3
pTyr
FGF-R3
A6-KMS11
NIH3T3
RPI-1 (μM) - 15 30 -
WCL
FGF-R3
actin
B
RPI-1 -
IP: FGF-R3
pTyr
FGF-R3
WCL
FGF-R3
actin
C
RPI-1(μM) - - 10 30
aFGF - + + +
pFGF-R
FGF-R3
pERKs
ERKs
pAKT
AKT
pSTAT3
STAT3
actin
D
RPI-1(μM) - 10 30
pJAK2
JAK2
pSTAT3
STAT3
actin

Fig. 2

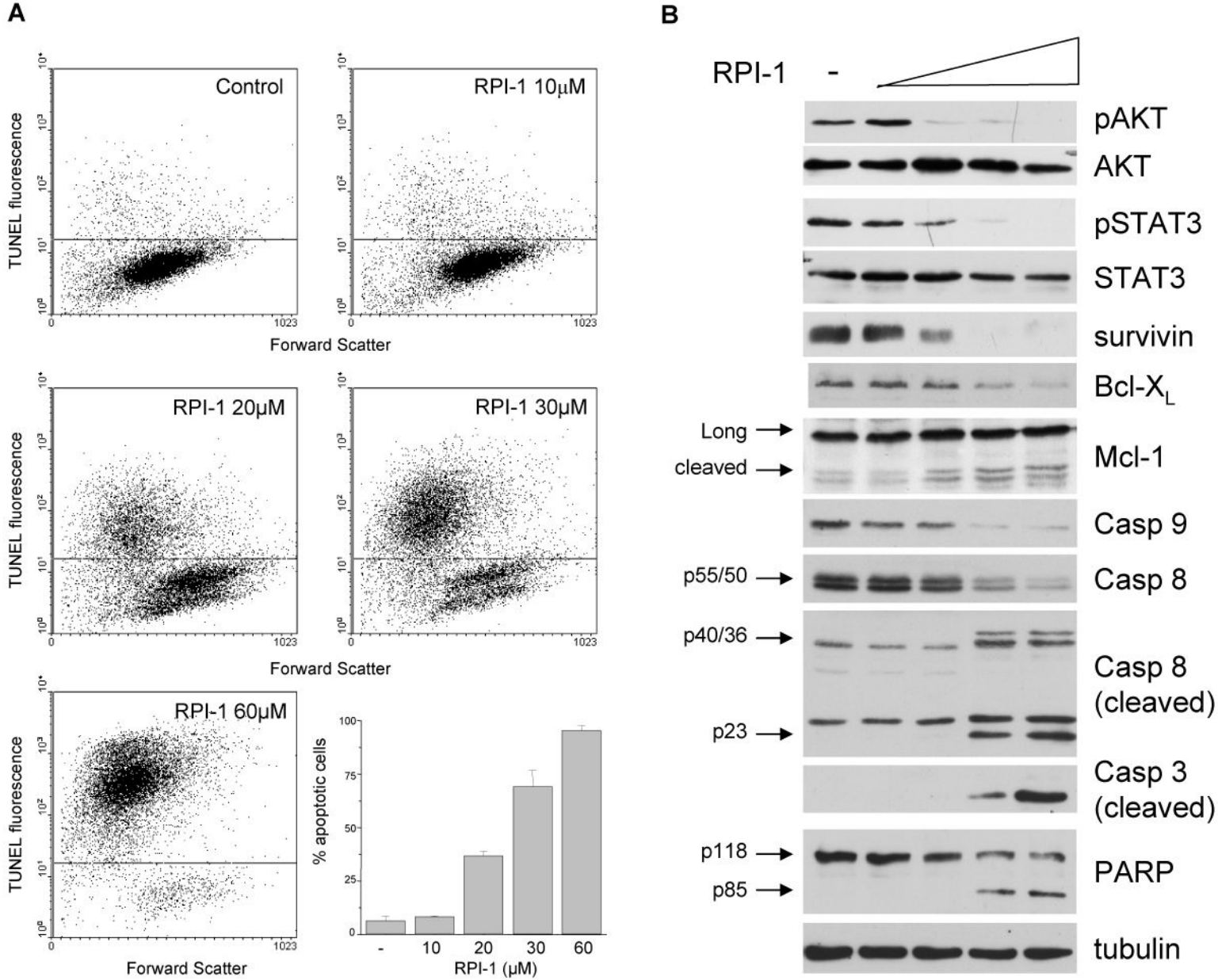
A
Control
RPI-1 10μM
RPI-1 20μM
RPI-1 30μM
RPI-1 60μM
TUNEL fluorescence
Forward Scatter
% apoptotic cells
RPI-1 (μM)
B
RPI-1
pAKT
AKT
pSTAT3
STAT3
survivin
Bcl-X_L
Long
cleaved
Mcl-1
Casp 9
p55/50
Casp 8
p40/36
p23
Casp 8 (cleaved)
Casp 3 (cleaved)
p118
p85
PARP
tubulin

Fig. 3

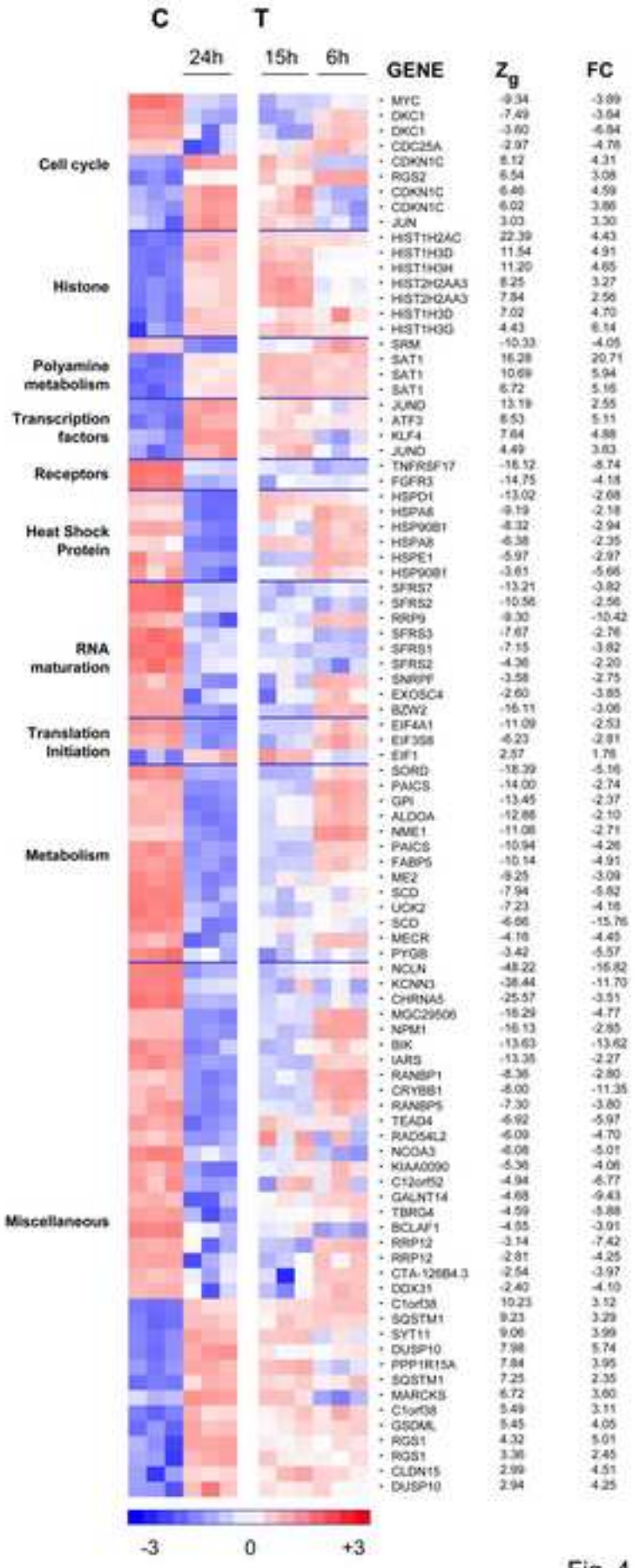

Fig. 4

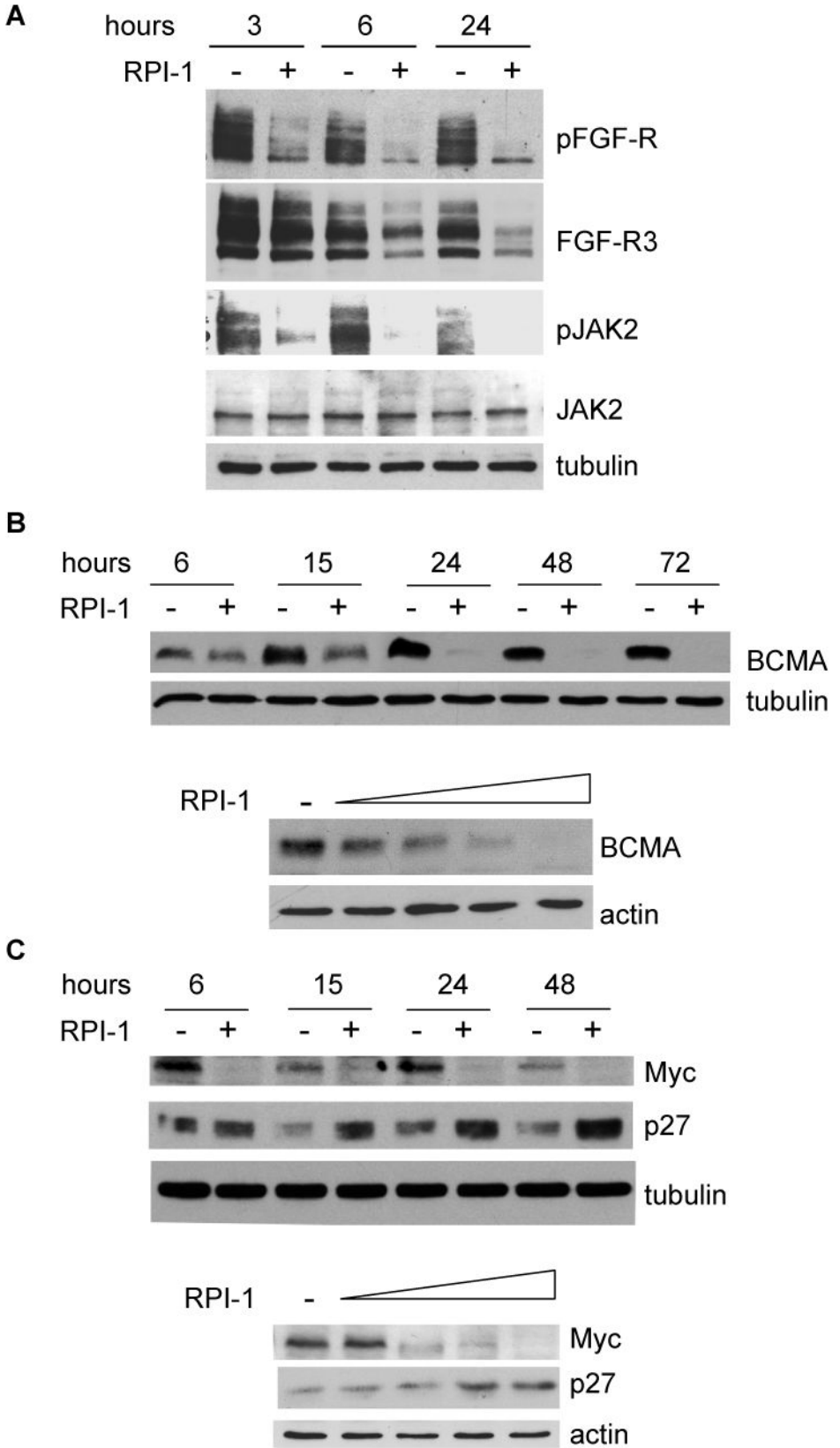
A
hours
3
6
24
RPI-1
- + - + - +
pFGF-R
FGF-R3
pJAK2
JAK2
tubulin
B
hours
6
15
24
48
72
RPI-1
- + - + - + - + - +
BCMA
tubulin
RPI-1
-
BCMA
actin
C
hours
6
15
24
48
RPI-1
- + - + - + - +
Myc
p27
tubulin
RPI-1
-
Myc
p27
actin

Fig. 5

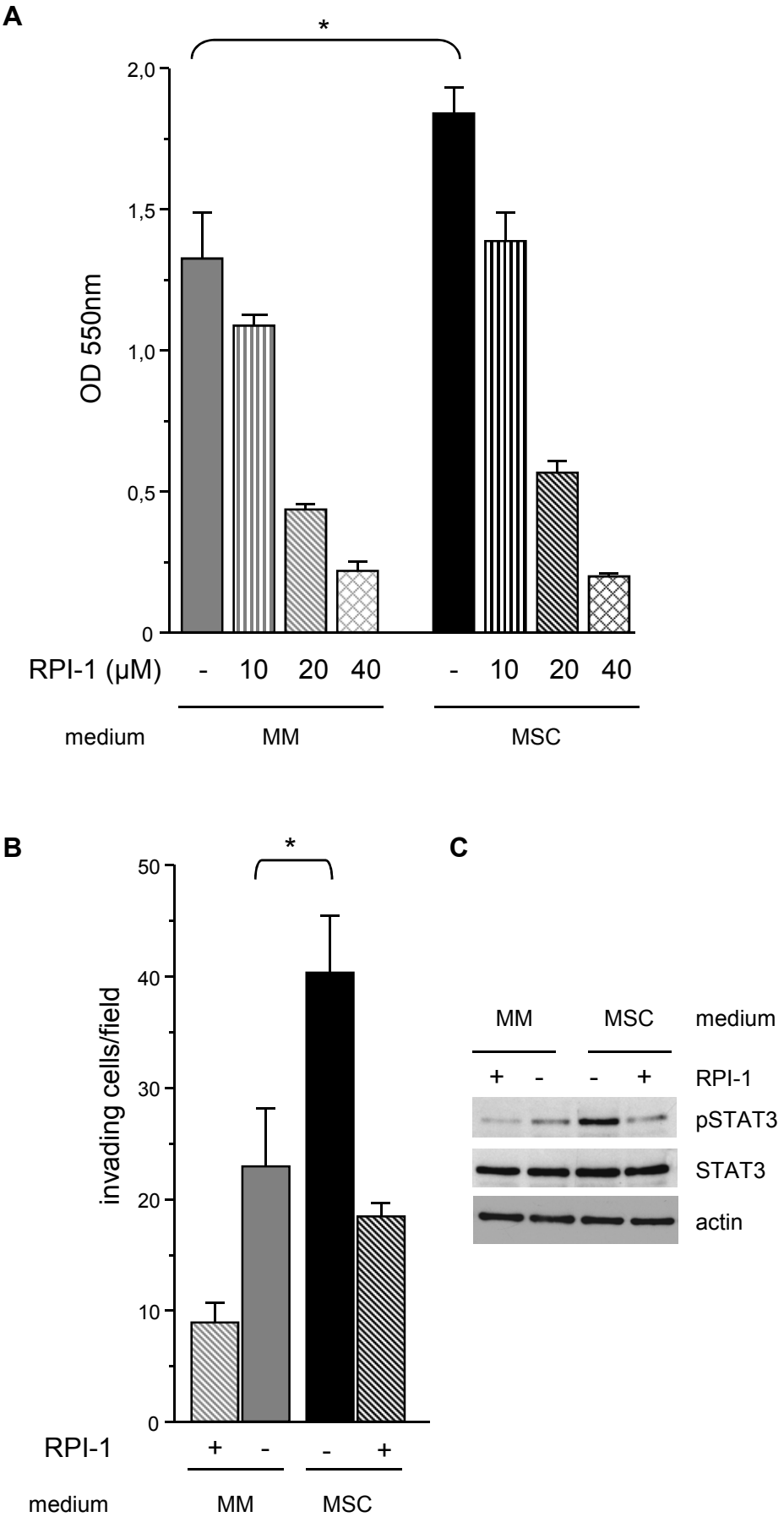

Fig. 6

Multiple pathways sustaining MM pathobiology are blocked by the multi-target tyrosine kinase inhibitor RPI-1

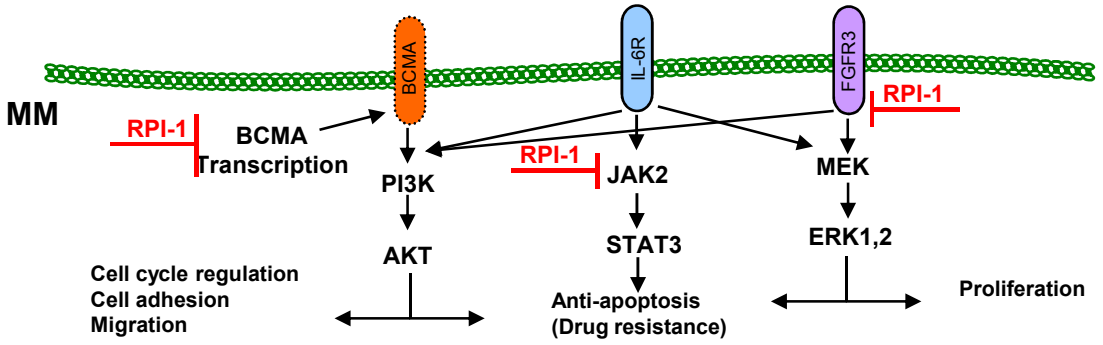

Cassinelli et al. Graphical Abstract